Clogging pressure of bubbles in microchannel contractions: theory and experiments

Mads Jakob Jensen*, Xiaolin Wang**, Daniel Attinger**, and Henrik Bruus*

* MIC - Department of Micro and Nanotechnology, Technical University of Denmark
DK-2800 Kongens Lyngby, Denmark, mjj@mic.dtu.dk
** Department of Mechanical Engineering, SUNY at Stony Brook
NY 11794-2300, USA, daniel.attinger@sunysb.edu

Abstract

We present a theoretical, numerical, and experimental study of bubbles passing through a microchannel contraction. A certain pressure, the so-called clogging pressure, is needed to push a bubble through a microchannel contraction. We present the first experimental results on such systems and compare them to results from a theoretical model first presented at NanoTech 2003 [1]. The experiments and theory are seen to be in quite good agreement and we give possible explanations for some of the discrepancies.

Keywords: microchannel, contraction, bubble, clogging

1 Introduction

Many microfluidic systems on modern lab-on-a-chip systems contain channel contractions. These tend to become problematic if gas bubbles are present in the system. If the bubbles are large enough and span the entire microchannel they are prone to get stuck at the channel contractions. Here they can block and/or disrupt the flow, and disrupt measurements in an uncontrolled manner. To drive the bubbles out of the channels a large external pressure is needed to be applied, this is the so-called clogging pressure. These problems were already identified a decade ago [2], [3] but never really studied in depth. Our goal with this work is to contribute to the solution of this technological problem by means of basic research.

We start by presenting the experimental set-up and describe the measurement method. Secondly, we give a short review of the theoretical and numerical model used. At last we compare and discuss the results of the two methods, and we give some concluding remarks.

2 Experiments

For the experimental part of the work different capillary glass tubes of circular cross section were used. The tubes were manufactured in the glass shop of Stony Brook University. The tubes have typical internal diameters $D = 2$ mm and a contraction diameter d ranging between 40 μm and 310 μm. One outlet of a given glass
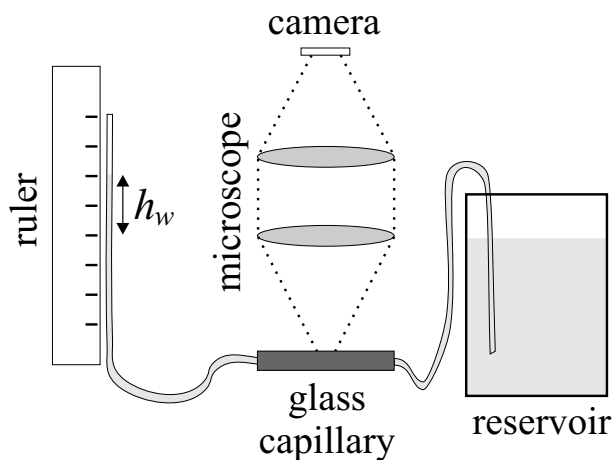

Figure 1: Experimental set-up used in the bubble clogging measurements. The height h_w of the water column is used to determine the pressure ΔP across the bubble. On Fig. 2 the detailed geometry of a bubble in the glass capillary is shown.

capillary is connected to a water reservoir and the other to a tube next to a scale, see Figs. 1 and 2. The connection tubes are made of Tygon. A hydrostatic pressure difference can then easily be applied and measured. A bubble is introduced into the system by shortly disconnecting one Tygon tube from the glass capillary and letting in air. Through a microscope (Edmundoptics, ST-2-0099, USA) the position of the left and right meniscus, x_L and x_R, respectively, is measured by taking pictures with the camera (1.3 megapixel, C-920 Zoom, Olympus, Japan), see Fig. 1. The position is hence found as a function of the applied pressure difference across the bubble $\Delta P = \rho g h_w$, where ρ is the density of water, g is the gravitational acceleration, and h_w is the water column height as sketched on Fig. 1.

While performing the experiments several precautions were taken as to ensure that the measurements were reproducible. Before any measurements: (1) distilled water is circulated in the tube in an ultrasonic bath for 5 minutes, (2) the water is then dried with clean compressed air (oil free). Neither solvents nor alcohol where put in the tubes as any residue might change
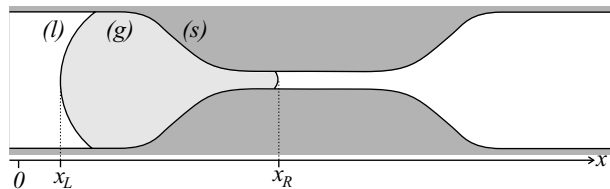
Figure 2: Schematic representation of the capillary where a gas bubble (g) in a liquid (l) is passing through the solid contraction (s). The left position x_L and right position x_R are marked as well as the zero point at the left of the bubble.

surface properties, e.g., the wetting angle.

As the measurements are to be compared with a theoretical model based on quasi-static assumptions, each measurement was performed when the system was in equilibrium. A 7 minutes delay between the setting of a new pressure point and the measurement allowed the bubble to reach its equilibrium position. Initial measurements with only tens of seconds of rest showed large discrepancies.

The experimental parameters that are used in the model are given in Table 1, together with estimates of the experimental error. Note that two different tubes have been used.

Table 1: Experimental values used in the theoretical model.

Variable	Value	Error	Tube Nr.
Contact angle	$\theta = 28°$	$\pm 4°$	All
Main	$D = 2.47$ mm	± 50 m	19
diameter	$D = 2.27$ mm	± 40 m	27
Restriction	$d = 110$ m	± 20 m	19
diameter	$d = 310$ m	± 20 m	27

3 Theory and Numerics

The theoretical and numerical part of the work is based upon an improved version of the model presented at NanoTech 2003 [1] (see also [4]). To apply and compare this model to the experiments one needs to: (a) to determine the shape $r(x)$ of the contraction (see Fig. 3) by tting a curve to the contraction shape captured by the camera, (b) to scale the shape according to the measured values of D and d (see Table 1), and (c) to import this shape into the computer program. The computer program then determines the pressure ΔP, the bubble length $L_{\text{bubble}} = x_R \quad x_L$, and the corresponding positions x_L and x_R.
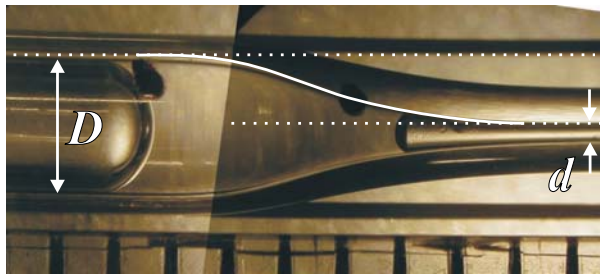

Figure 3: Images of the channel contraction taken by the camera depicted in Fig. 1. The images are used to make a curve t and so determine the shape $r(x)$ of the contraction.

The model assumes quasi-static motion of the bubble. This implies that the contact angle θ between the liquid-gas interface and the solid-liquid interface is constant. An estimate of the maximal clogging pressure is given by the pressure required to move the bubble in a so-called sudden contraction

$$\Delta P_{\max} = 4 \quad \cos\theta \quad \frac{1}{d} \quad \frac{1}{D} \quad , \qquad (1)$$

where is the liquid-gas surface tension. In the case of real physical systems as in our experiment the contact angle θ actually show some hysteresis. The contact angle has different values when receding θ_R and advancing θ_A. These different angles are due to different local wetting phenomena and contact line pinning [5].

4 Discussion and Conclusion

In the following we will only study two out the 27 glass tubes we have manufactured. They are referred to as tube 19 and tube 27.

On Figs. 4 and 5 the experimental data for tube 19 is compared to the results of the simulations. On these two rst graphs the results are shown for a large bubble (full line) and a small bubble (dotted line), respectively. The experimental data is represented with error-bars.

Figure 4 depicts the pressure ΔP across the bubble as a function of the position of the left meniscus x_L. It should here be pointed out that the position is measured from different zero points, whence the different location of the two graphs. The pressure is seen to increase very rapidly. When the right side of the bubble x_R enters the contraction it advances rapidly compared to the left side x_L because of mass conservation. Moreover, most of the pressure drop is across the small meniscus having the largest curvature ($\propto 1/d$).

On Fig. 5 the length of the bubble L_{bubble} is shown as function of the pressure across the bubble. From this gure it is clear that the solid line represents the longer bubble.

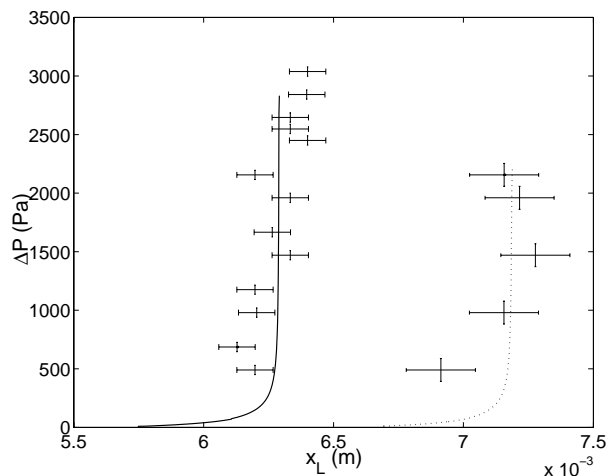Figure 4: For tube 19: the pressure ΔP across the bubble as a function of the position of the left meniscus x_L. The figure includes: (a) the dots are experimental data, (b) the full line is the model calculation for a large bubble, and (c) the doted line similarly for a small bubble.
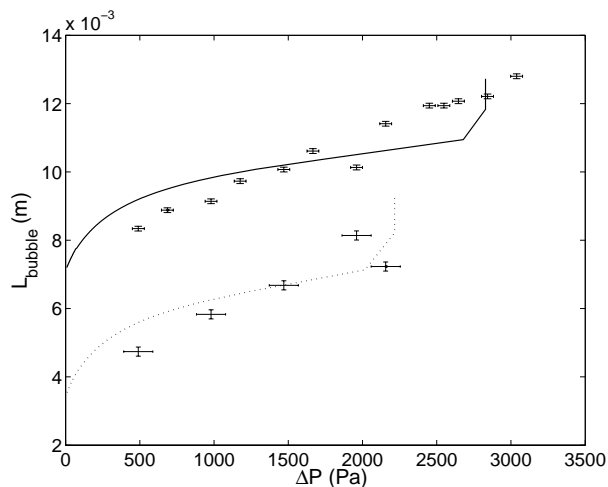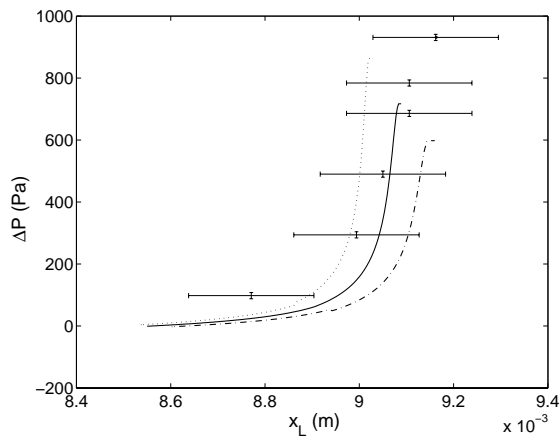

Figure 6: For tube 27: the pressure ΔP across the bubble as a function of the position of the left meniscus x_L. The figure includes: (a) experimental data (dots), and theoretical calculations using (b) the mean measurements of θ, D and d as input (full line) and (c) the largest deviation for $\theta \pm 4°$, $d \pm 20$ m, and $D \pm 40$ m (dotted lines).

Figure 5: For tube 19: the length of the bubble $L_{\text{bubble}} = x_R - x_L$ as a function of the pressure across the bubble ΔP. The figure includes: (a) dots representing experimental data, and model calculations for (b) a large bubble (full line) and (c) a small bubble (dotted line).

On Figs. 6 and 7 the experimental data for tube 27 is compared to the results of the simulations. For clarity we have chosen to present data only for a large bubble. In this case the dotted graphs represent numerical simulations where the parameters d, D, and θ have been chosen as the maximum and minimum of the deviations shown in Table 1.
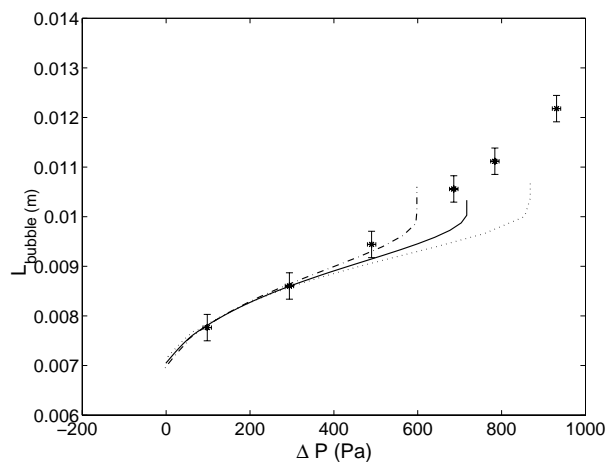

Figure 7: For tube 27: the length of the bubble $L_{\text{bubble}} = x_R - x_L$ as a function of the pressure across the bubble ΔP. The figure includes: (a) dots (experimental data), and theoretical calculations using (b) the mean measurements of θ, D and d as input (full line) and (c) the largest deviation $\theta \pm 4°$, $d \pm 20$ m, and $D \pm 40$ m (dotted lines).

As a general trend the data is seen to be in relatively good agreement with the numerical model. However, it is seen from Figs. 4 and 6 that the measured pressures generally are larger than the ones predicted by the model. This might be tentatively explained by the contact angle hysteresis mentioned earlier. On slightly

contaminated surfaces the advancing angle θ_A is larger than the receding angle θ_R [5]. If we consider the measurements near the the maximum pressure, when the bubble is moving towards the right, the following might happen: the meniscus in the large part of the channel stops advancing with a contact angle slightly larger than θ, while the side in the restriction stops with a slightly smaller angle than θ. If we assume that $\theta_A = \theta + 10°$ and $\theta_R = \theta - 10°$ we may use the model equation Eq. (1) to give an estimate of the ratio between the experimental (with hysteresis) and the theoretical maximal pressures (without hysteresis):

$$\text{ratio} = \left(\frac{\cos\theta_R}{d} - \frac{\cos\theta_A}{D}\right)\left(\frac{\cos\theta}{d} - \frac{\cos\theta}{D}\right)^{-1}, \quad (2)$$

for typical values used in this project this ratio is about 1.1 meaning that the experimentally measured values are larger. This is exactly the trend seen.

Another source of possible error lies in the fact that the initial volume of the bubble is a parameter in the simulations. This initial value was not determined experimentally and a shooting method was used to fit the correct initial volume. Finally, it should be mentioned that the glass capillaries were not perfectly symmetric which was assumed in the program. This last fact would however not have a vary large influence on the results.

In conclusion it is obvious that although the model does not catch all the details of the experiments, like surface related effects such as wetting and pinning of the contact line, it does in general yields good results which are within 10% of the measurements. As such the model is a good design tool that may be used in, e.g., the development of micro fluidic systems. Most importantly this work is one of the first combined experimental, theoretical, and numerical studies which is tackling the problem of bubble clogging in microchannel contraction.

REFERENCES

[1] M. J. Jensen, G. Goranović, and H. Bruus, NanoTech 2003, San Francisco, USA, February 2003, proc. vol. **1**, p. 258-261.

[2] P. Gravesen, J. Branebjerg, and O. Søndergård Jensen, J. Micromech. Microeng. **3**, 168 (1993).

[3] M. Elwenspoek, T. S. Kannerubj, R. Miyake, and J. H. J. Fluitman, J. Micromech. Microeng. **4**, 227 (1994).

[4] M. J. Jensen, G. Goranović, and H. Bruus, J. Micromech. Microeng., (submitted 2003), www.mic.dtu.dk/research/MIFTS/publications

[5] P. G. de Gennes, Rev. Mod. Phys. **57**, 827 (1985).